RESEARCH ARTICLES

HGT

Adeno-Associated Virus Capsid-Promoter Interactions in the Brain Translate from Rat to the Nonhuman Primate

Martin O. Bohlen,[1,†] Thomas J. McCown,[2–4,†] Sara K. Powell,[4,5] Hala G. El-Nahal,[1] Tierney Daw,[1] Michele A. Basso,[6] Marc A. Sommer,[1,7,8] and R. Jude Samulski[4,9,*]

[1]Department Biomedical Engineering, Duke University, Durham, North Carolina, USA; Departments of [2]Psychiatry, [3]Pediatrics, and [9]Pharmacology, University of North Carolina at Chapel Hill, Chapel Hill, North Carolina, USA; [4]UNC Gene Therapy Center, University of North Carolina, School of Medicine, Chapel Hill, North Carolina, USA; [5]Asklepios Biopharmaceutical, Inc., Research Triangle Park, NC, USA; [6]Fuster Laboratory of Cognitive Neuroscience, Department of Psychiatry and Biobehavioral Sciences and Neurobiology, and Jane and Terry Semel Institute for Neuroscience and Human Behavior, Brain Research Institute—David Geffen School of Medicine, University of California Los Angeles, Los Angeles, California, USA; [7]Department of Neurobiology, Duke University School of Medicine, Durham, North Carolina, USA; [8]Center for Cognitive Neuroscience, Duke University, Durham, North Carolina, USA.
[†]These authors contributed equally to this work.

Recently, we established an adeno-associated virus (AAV9) capsid-promoter interaction that directly determined cell-specific gene expression across two synthetic promoters, Cbh and CBA, in the rat striatum. These studies not only expand this capsid-promoter interaction to include another promoter in the rat striatum but also establish AAV capsid-promoter interactions in the nonhuman primate brain. When AAV serotype 9 (AAV9) vectors were injected into the rat striatum, the minimal synthetic promoter JetI drove green fluorescent protein (GFP) gene expression predominantly in oligodendrocytes. However, similar to our previous findings, the insertion of six alanines into VP1/VP2 of the AAV9 capsid (AAV9AU) significantly shifted JetI-driven GFP gene expression to neurons. In addition, previous retrograde tracing studies in the nonhuman primate brain also revealed the existence of a capsid-promoter interaction. When rAAV2-Retro vectors were infused into the frontal eye field (FEF) of rhesus macaques, local gene expression was prominent using either the hybrid chicken beta actin (CAG) or human synapsin (hSyn) promoters. However, only the CAG promoter, not the hSyn promoter, led to gene expression in the ipsilateral claustrum and contralateral FEF. Conversely, infusion of rAAV2-retro-hSyn vectors, but not rAAV2-retro-CAG, into the macaque superior colliculus led to differential and selective retrograde gene expression in cerebellotectal afferent cells. Clearly, this differential promoter/capsid expression profile could not be attributed to promoter inactivation from retrograde transport of the rAAV2-Retro vector. In summary, we document the potential for AAV capsid/promoter interactions to impact cell-specific gene expression across species, experimental manipulations, and engineered capsids, independent of capsid permissivity.

Keywords: AAV, promoter, nonhuman primate, capsid, retrograde

INTRODUCTION

Adeno-associated virus (AAV) vectors have achieved a prominent position in central nervous system (CNS) clinical trials, particularly with respect to the use of AAV serotype 9 (AAV9) for single gene disorders, such as spinal muscular atrophy and giant axon neuropathy.[1,2] From a basic research perspective, many AAV vectors have been used to target precise neuronal populations for optogenetic and chemogenetic manipulation, an approach that has revealed complex neuroanatomical connections and novel insights into functional dynamics.[3–6] In general, achieving cell-selective transduction and gene expression has involved manipulation of the AAV capsid and utilization of cell-specific promoters or enhancers,[7–10] where these elements have been thought to be mutually exclusive.

Recently, however, we established that the AAV9 capsid exhibits a previously unknown novel property within the rodent CNS, namely the ability of a capsid-promoter interaction to influence cell-specific transgene expression *in vivo*.[11] Using identical transgene cassettes packaged in the AAV9 capsid, the chimeric CMV-chicken ß-actin promoter, CBA, supported dominant neuronal gene expression in the rat striatum, while a truncated CBA promoter, a novel hybrid form of the CBA promoter, CBh, exhibited a significant shift in transgene expression to oligodendrocytes. Moreover, six glutamate or six alanine

*Correspondence: R. Jude Samulski, UNC Gene Therapy Center, CB7352, University of North Carolina School of Medicine, Chapel Hill, NC 27599, USA. E-mail: rjs@med.unc.edu

insertions into capsid proteins VP1/VP2 reversed the anticipated cellular transgene expression driven by CBA or CBh, respectively.

Although these studies provide the first demonstration of an AAV capsid-promoter interaction that influences cell type-specific expression, the general principle of a capsid-promoter interaction could explain divergent results from previous studies. For example, Haberman *et al.*[12] reported that two AAV vectors with similar promoters driving therapeutic gene expression exhibited diametrically opposed results with regard to *in vivo* seizure attenuation. When therapeutic gene expression was driven by a CMV promoter containing a CMV immediate early enhancer, *in vivo* seizure sensitivity was significantly attenuated. When the same therapeutic gene expression was driven by a minimal CMV promoter (without enhancer) in the context of a TET-off element, *in vivo* seizure sensitivity was significantly heightened. The basis for this dichotomy was revealed by mixing the two rAAV2 vectors where CMV drove LacZ expression and Tet-OFF-CMV drove green fluorescent protein (GFP) expression. After CNS infusion, 41% of the transduced neurons expressed GFP alone, 24% expressed LacZ alone, and 35% were positive for both reporter genes. In light of our recent demonstration of an AAV capsid-promoter interaction,[11] these findings by Haberman *et al.*[12] could be reinterpreted to support the proposition that an rAAV2 capsid interaction with one or both of the promoters caused divergent patterns of neuronal gene expression.

Given that numerous AAV capsid libraries utilize constitutive or cell type- specific promoters as part of the selection criteria,[7] we aimed to expand on previously reported capsid-promoter interactions in rats and determine whether this phenomenon translates to the nonhuman primate brain. We report that, as with the CBA and Cbh promoters, the AAV9 capsid also interacts with the JetI synthetic promoter[13] to alter cellular transgene expression in the rat brain. Also, based upon the recent observation of a AAV capsid-promoter interaction,[11] we decided to retrospectively look for potential evidence of this interaction across viral injections made in primates. For this, we aggregated primate neuroanatomical data from two laboratories, whose focus was on a single capsid, rAAV2-Retro, with injections placed within the well-understood visuomotor circuitry of the primate brain. From the available data, we were able to make revealing comparisons, where rAAV2-Retro carrying either the human synapsin (hSyn) or a hybrid chicken beta actin (CAG) promoter was infused into either the macaque frontal eye field (FEF) or superior colliculus (SC). In general, the neuroanatomical underpinnings of these visuomotor structures are phylogenetically conserved and their connectivity has been established across a broad number of species using autoradiographic and conventional tracers. Thus, retrograde transduction patterns were compared across viral injections using the well-established afferent connections with the FEF[14–16] and SC[17–21] in monkeys. Results from both species supported the hypothesis that cell-specific capsid-promoter interactions influence cellular transgene expression following retrograde transport. These findings provide a potential explanation for conflicting *in vivo* neural circuit expression patterns in previous experiments that involved different promoters[22] and AAV capsids and point to the importance of considering capsid-promoter interactions in translation to clinical applications. Finally, these findings raise questions regarding the basis for cellular specificity of many engineered chimeric AAV capsids, as well as the more extensively studied conventional AAV capsids.

MATERIALS AND METHODS

Rodents

Rodent virus production. Viruses were produced in HEK293 cells as previously described.[23] Briefly, polyethylenimine max was used for the triple transfection of a cap and rep plasmid (pGSK2/9 and pGSK2/9AU), the pXX6-80 helper plasmid, and the transgene plasmid (pJetI-GFP, gift from Dr. Steve Gray, UT Southwestern). Cells were harvested 48 h post-transfection, and the virus was purified by cesium chloride ultracentrifugation. After identifying peak fractions by quantitative polymerase chain reaction (qPCR), the virus was dialyzed into $1\times$PBS/NaCl/D-Sorbitol. Titers were calculated by qPCR according to established procedures using a LightCycler 480 instrument and ITR primers. The individual titers were 2.9×10^{11} vector genomes/mL for scAAV9-JetI-GFP and 8.4×10^{11} vector genomes/mL for scAAV9AU-JetI-GFP.

Animals and stereotactic infusions. All the animals included in this study were male Sprague-Dawley rats (Charles River Laboratories) weighing between 200 and 300 g at the time of intracranial injections. Animals were maintained on a 12-h light/12-h dark cycle and had free access to water and food. Animal care and surgical procedures were in accordance with the NIH Guide for the Care and Use of Laboratory Animals, and all procedures received prior approval by the University of North Carolina Institutional Animal Care and Usage Committee and with the approval of the University of North Carolina Institutional Review Board.

Virus vector infusions were performed as previously described.[23] First, animals were anesthetized using pentobarbital (50 mg/kg, IP) and placed into a stereotactic frame. Using a 32G stainless steel injector and a Hamilton infusion pump, animals received 3 μL of each vector over 15 min into each side of the striatum (0.5 mm anterior to bregma, 3.5 mm lateral, and 5.5 mm vertical, according to the atlas of Paxinos and Watson[24]). The injector was then left in place for 3 min postinfusion, to allow time for the virus to diffuse from the injection site.

Histology and microscopy. Two weeks after AAV vector infusion, animals received an overdose of pentobarbital

(100 mg/kg, IP), and they were perfused transcardially with ice-cold 100 mM phosphate-buffered saline (PBS) (pH 7.4), followed by 4% paraformaldehyde in PB (pH 7.4). Brains were postfixed 12–48 h at 4°C in the paraformaldehyde-PB, and 40-μm coronal sections were cut using a vibrating blade microtome for subsequent immunofluorescence.

To determine fluorescent transgene (GFP) cellular co-localization, tissue sections were incubated in a blocking solution with one of these cellular marker antibodies: NeuN (1:500; Chemicon), Olig2 (1:250; Abcam), or GFAP (1:2000; Dako). Following incubation at 4°C for 48–72 h in primary antibodies, the sections were rinsed thrice with PBS and blocked again for 45 min at room temperature. Subsequently, the tissue sections were incubated in either Alexafluor 488 or 594-conjugated goat anti-rabbit IgG or goat anti-mouse (Invitrogen) (diluted 1:500 in 10% goat serum/PBS) for 1 h at 4°C. Rinsed sections were mounted, and fluorescence was visualized using an Olympus FV3000RS confocal microscope in the UNC Neuroscience Center Microscopy Core. Transgene fluorescence co-localization was determined on the *z* stacks. Individual GFP-positive/marker-positive cells were counted across four sections separated by 80 μm for each vector condition. Significant differences between the total number of neuron or oligodendrocyte-positive cells were determine by a two-tailed Students *t*-test.

Primates

Viral vectors. Viral vectors were purchased from commercial sources. Titers, injection locations, and parameters are reported in Table 1.

Animals and stereotactic infusions. All methods were approved by either the University of California, Los Angeles, or Duke University IACUCs and were performed in accordance with the NIH *Guidelines for Animal Care and Use* and with the approval of both universities Institutional Review Boards.

FEF injections. Case 1 participated in transcranial electric and magnetic stimulation studies.[25–28] In Cases 1–3, animals received a prophylactic dose of corticosteroids (Dexamethasone [2.0 mg/kg, IM] or Solu-Medrol [15.0 mg/kg, IM]) the day before surgery and this dosage was tapered over 2 weeks, postoperatively. On the surgery date, animals were sedated with ketamine hydrochloride (3.0 mg/kg, IM) and Dexdomitor (0.075 mg/kg, IM), and then intubated. An anesthetic plane was subsequently maintained for the duration of surgery using a 1–3% isoflurane/oxygen mix.

The animal was placed into a stereotaxic apparatus (Kopf Instruments, Tujunga, CA). All surgical procedures were carried out under aseptic conditions. The scalp was thoroughly cleaned using betadine and chlorhexidine scrubs, followed by 200 proof ethanol. During surgery, vital signs were monitored and maintained within normal limits by a trained veterinary technician. Before an incision was made and after final suturing, a cutaneous injection of 0.25% Bupivacaine (0.5–1.0 mL/<4 mg) was administered along the incision line.

For FEF injections, a midline incision was made and soft tissues were retracted to visualize the skull. Using stereotaxic coordinates, a hole was trephined above the FEF. A durotomy was performed to visualize the underlying cortex. A Hamilton syringe was held in a micromanipulator at either a 90° angle (Table 1; Case 1) with respect to the horizontal plane or at a 45° angle (Table 1; Case 2 and 3), with the tip angled medially. The surface of the FEF sits at $\sim$45° in the horizontal plane; thus, by angling the needle at 45°, the track was orthogonal to the cortical surface. For Cases 1 and 3, the needle was advanced $\sim$5 mm from the surface, where 2 μL of rAAV2-Retro was deposited at $\sim$1 μL/min rate. The solution was allowed to diffuse from the injection site for 5 min. Next, the syringe was drawn up 1 mm and another 1–2 μL injection was made, followed by a second 5-min waiting period before withdrawing the needle. This procedure was replicated at multiple sites along the genu of the arcuate sulcus. For Case 2, the needle was advanced to $\sim$5 mm from the cortical surface, then drawn up 2 mm and a single 5 μL injection was made at 0.5 μL/min within the FEF.

Following injections, the dura was sutured back together, and the bone flap was replaced; then the muscle was sutured back to its insertion points. Finally, the skin was reapproximated with suture. For postoperative analgesia, animals received one dose of buprenorphine SR (0.2 mg/kg, IM).

Table 1. *Basic monkey parameters*

Case: Lab ID	*Species*	*Injection Site*	*Construct*	*Source*	*Titer (vg/mL)*	*Injection Volume (μL)*	*Expression Latency (Days)*
1: M17-04	Rhesus Macaque	FEF (Broadman Area 8)	rAAV2-Retro-CAG-GFP	UNC	1.8×10^{12}	18	28
2: M20-01	Cynomolgus Macaque	FEF (Broadman Area 8)	rAAV2-Retro-CAG-tdTomato	UNC	2.6×10^{12}	5	147
3: M19-03	Cynomolgus Macaque	FEF (Broadman Area 8)	rAAV2-Retro-hSyn-hChR2(H134R)-EYFP	AddGene	1.1×10^{13}	20	64
4: M19-07	Rhesus Macaque	SC	rAAV2-Retro-CAG-GFP	UNC	1.8×10^{12}	3	51
5: M20-02	Rhesus Macaque	SC	rAAV2-Retro-CAG-tdTomato	UNC	3.8×10^{12}	3	98
6: M18-11	Rhesus Macaque	SC	rAAV2-Retro-hSyn-hChR2(H134R)-GFP	Salk	2.5×10^{13}	9	264

FEF, frontal eye field; SC, superior colliculus.

SC injections. Cases 4–6 were involved in prior psychophysical and electrophysiological studies.[29–31] Thus, these animals had existing chambers, which provided access to the SC. Using electrophysiologically identified coordinates, a 10 μL Hamilton syringe or a custom injectrode was used to inject a total of 3 μL at 0.1 μL/min in a single location within the SC (Case 4 and 5) or 9 μL at 0.1 μL/min in three locations throughout the SC (Case 6). At each site, a 1 μL injection was made at three depths.

Histology and microscopy. Following a survival period (Table 1), animals were sedated with ketamine hydrochloride (3.0 mg/kg, IM) and then deeply anesthetized with sodium pentobarbital (50.0 mg/kg, IP). Once the animals were totally areflexic, they were transcardially perfused with 2–4 L of chilled 0.1 M, pH 7.4 PBS, followed by 4 L of 4% paraformaldehyde in 0.1 M, pH 7.4 PBS. Next, the brain was blocked in the frontal plane using a stereotaxic apparatus and postfixed in 4% paraformaldehyde in 0.1 M, pH 7.4 PBS, at 4°C for 24–48 h. Blocks were then cryoprotected in 30% sucrose at 4°C. Afterward, blocks were cut using a freezing stage, sliding microtome (American Optical Company, Buffalo, NY), and sections were stored in PBS at 4°C.

For immunofluorescence amplification, free-floating sections were incubated in immunoblocking serum consisting of 1% bovine serum albumin/0.1% Triton X-100 in PBS for 2 h at room temperature. Following a rinse, sections were incubated in rabbit anti-GFP in PBS (1:200; #5450, Abcam) for 24–48 h at 4°C. Next, sections were rinsed and placed in a secondary antibody solution consisting of 1:385 donkey anti-rabbit IgG antibody conjugated to Alexa Fluor 488 (#705-545-147; Jackson ImmunoResearch) in 2% normal donkey serum in PBS for 2 h at room temperature.

For immunohistochemical visualization of the green fluorescent family of proteins, a detailed protocol has previously been published.[32] Briefly, free-floating sections first underwent a blocking step to inhibit endogenous peroxidase activity. Sections were moved to a 0.25% solution of Triton X-100 in PBS, and then transferred to a 1% BSA/0.25% Triton X-100 in PBS solution. They were incubated in biotinylated goat anti-GFP ($\sim$1:200; 600-106-215; Rockland) in a 1% BSA/0.25% Triton X-100 in PBS solution for 1–3 h at room temperature, followed by $\sim$24–48 h at 4°C. After being rinsed in PBS, they were incubated in biotinylated rabbit anti-goat IgG secondary antibody (PK6105; Vector Laboratories) for 1.5 h at room temperature. Sections were then transferred to an avidin-biotin-horseradish peroxidase complex (ABC) solution (PK6105; Vector Laboratories) for 1 h at room temperature. Following another 15-min PBS wash, sections were placed in 0.5% diaminobenzidine (DAB)/0.01% cobalt chloride/0.01% nickel ammonium sulfate in PBS solution for 20 min. Subsequently, 0.3% H_2O_2 was added and allowed to react with the DAB for 15–30 min to produce a dark brown-black reaction product in locations where cells contained the fluorescent protein. Sections were then mounted on gelatinized glass slides and left to air dry overnight. Dry mounted sections were counter stained with thionin. In all cases, sections were then dehydrated in graded alcohol baths and coverslipped using Cytoseal 60.

Sections were drawn using a Bausch & Lomb microprojection microscope for structural anatomy, and then a Zeiss AxioImager 2 with an affixed drawing tube was used to plot the locations of labeled cells over the anatomical drawing. For one case (Case 5), the only available tissue was fluorescence. Sections from this case were scanned using a Zeiss Axioscan. The digital scan of the entire section was imported into CorelDRAW 2020 (Corel Corp., Ottawa, Canada), in which the anatomical outlines were drawn and the locations of labeled cells were marked. Brightfield and fluorescent photomicrographs were taken using a Zeiss Axio Scan.Z1.

RESULTS

AAV9 capsid interactions with a synthetic promoter determine cellular transgene expression in the rat striatum

Even though Powell *et al.*[11] established that the AAV9 capsid exhibits a direct interaction across the CBA and Cbh promoters, the possibility remained that the interactions were unique to these two similar promoters. Therefore, we tested the influence of the AAV9 capsid on a synthetic JetI promoter[13] driving cellular transgene expression of GFP in the rat striatum. Rats received a 3 μL infusion of AAV9-JetI-GFP or the AAV9AU-JetI-GFP where six alanines had been inserted into amino acid 139 of AAV9 VP1/VP2. Two weeks later, the rats were perfused and the brains were sectioned, processed immunohistochemically, and the region containing the injection site was analyzed.

As seen in Fig. 1A–C, the green AAV9-JetI GFP expression is prominent in oligodendrocytes identified by the red fluorescent marker for anti-Olig2 (34 $\pm$ 4 Olig2-positive cells/section). By comparison, relatively few neurons co-localized with the red fluorescent marker attached to anti-NeuN (17 $\pm$ 4 NeuN-positive cells per section) (Fig. 1D–F). In marked contrast, the insertion of six alanine residues into AAV9 VP1/2 (AAV9AU) significantly altered the AAV9-mediated cellular expression pattern. Figures 1G–I show that there are numerous green fluorescing GFP neurons that co-localize with the red anti-NeuN signal (67 $\pm$ 5 NeuN-positive cells/section), while the number of GFP-positive cells co-localizing with red anti-Olig2-positive oligodendrocytes remained similar to that after AAV9 transduction (Fig. 1J, K) (32 + 2 Olig2-positive cells). Supplementary Figure S1 shows that the AAV9AU vectors significantly increased the total number of GFP-NeuN-positive cells versus AAV9 vectors, but did

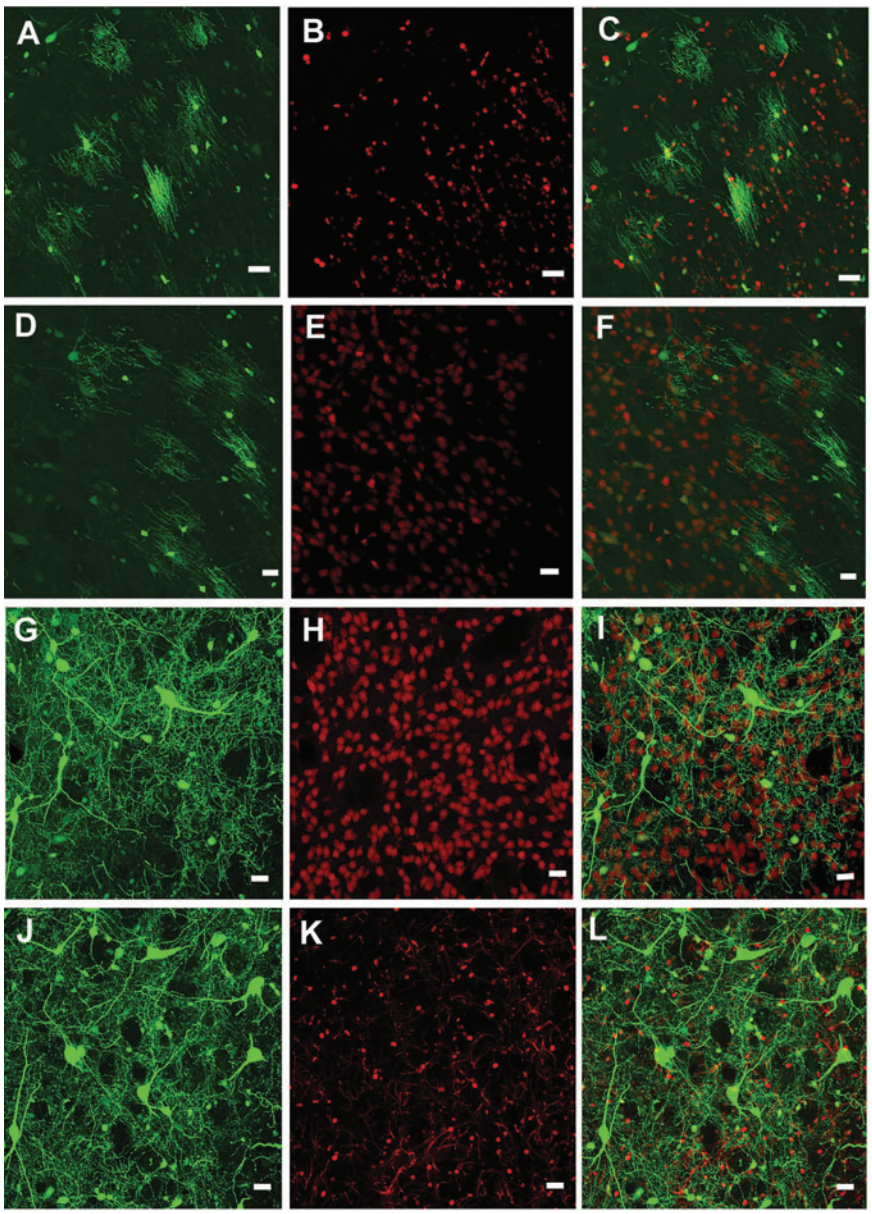

Figure 1. Confocal images of AAV9-hSyn and AAV9AU-hSyn mediated transduction in the rat striatum. **(A–C)** AAV9-JetI-GFP gene expression primarily co-localizes with the oligodendrocyte marker, Olig2, while **(D–F)** the general lack of GFP co-localization is with the neuronal marker, NeuN. In contrast **(G–I),** AAV9AU-JetI-GFP gene expression exhibits substantial co-localization with NeuN, but little co-localization with Olig2. Scale bars equal 20 μm. AAV, adeno-associated virus; GFP, green fluorescent protein.

not alter the total number of GFP-Olig2-positive cells. This influence of the AAV9AU capsid on cellular GFP expression agrees with a similar shift in cellular transgene expression we observed in the context of the CBh promoter.[11] No astrocyte co-localization was found for either promoter (Supplementary Fig. S2). Thus, the data show that the AAV9 capsid directly influences cellular transgene expression from another constitutive, synthetic promoter in the rat striatum. We anticipate that these phenomena are more widespread than the limited number of cassettes and capsids we have selected. Given a number of disparate findings for nonhuman primate investigations,[22] we therefore conducted retrospective studies on visual field AAV transduction in nonhuman primates.

rAAV2-Retro promoter-dependent FEF retrograde transgene expression in the nonhuman primate

The rAAV2-Retro vector has provided a powerful tool for neuronal circuit investigations in the CNS across a number of species.[10,33] This study investigated the pattern of retrograde labeling with rAAV2-Retro using either a constitutive promoter, CAG, or a neuron-specific promoter, hSyn. Retrograde transduction patterns were com-

pared across injections using the well-established afferent connections with the FEF in monkeys.[14–16] Intraparenchymal infusion of rAAV2-Retro-CAG-GFP, rAAV2-Retro-CAG-tdTomato, or rAAV2-Retro-hSyn-hChR2(H134R)-EYFP into the FEF resulted in substantial, local neuronal labeling (determined when labeled somata were within the plane of section) within the injected FEF (Figs. 2A, E; 3A–C; 4A, E, and I). In all three cases, a limited number of retrogradely labeled neurons were observed within the ipsilateral cingulate gyrus (Figs. 2A, D, E and 3B, C) and ipsilateral supplementary eye field (Figs. 2A, D, E; 3B, C; 4D, H, L). However, a comparison of transduction patterns between the different promoters revealed unanticipated stark differences. The rAAV2-Retro-CAG-GFP produced retrograde labeling of a large number of neurons within the claustrum (Figs. 2A–C, D, E and 4B, F). It also retrogradely labeled corticocortical neurons within the FEF contralateral to the injection site (Figs. 2A, B, D, E and 4C, G). In contrast, injections of rAAV2-Retro-hSyn-hChR2(H134R)-EYFP failed to provide the same pattern of neuroanatomical expression within either the claustrum (Figs. 3A–D and 4J) or the contralateral FEF (Figs. 3A–C and 4K). In addition, all the injected vectors failed to show strong evidence of transgene expression within thalamocortical neurons in the mediodorsal thalamus, a well-established connection to the FEF.[16,34,35] These results are summarized in Table 2 and extend our rodent observations of capsid-/promoter-specific expression profiles to the nonhuman primate animal model.

Promoter-dependent SC retrograde transgene expression in the nonhuman primate

The cerebellotectal connection is phylogenetically conserved and well established using autoradiographic and conventional tracer techniques (Rat[17]; Squirrel[19]; Cat[20,21]; Monkey[18]). Furthermore, the SC is a second important locus in the control of eye movements, so injections of rAAV2-Retro constructs carrying either the hSyn or CAG promoters were placed into the SC of three monkeys. Following electrophysiological mapping of the SC, a small injection of rAAV2-Retro-CAG-GFP or rAAV2-Retro-CAG-tdTomato was placed caudally within the SC of two animals (Figs. 5B, E and 7B, E), and multiple injections of rAAV2-hSyn-hChR2(H134R)-GFP were made in the colliculus of a third animal (Figs. 6B and 7H). Anatomical assessment of transduction revealed local neuronal labeling around the injection sites for all three cases (Figs. 5B, E; 6B; and 7B, E, H). Inspection of the FEFs from all three cases revealed the presence of retrogradely labeled corticotectal neurons within the FEF ipsilateral to the injection site (Figs. 5A, D; 6A; and 7A, D, G). In addition, in Case 6, the likely combination of the larger injection volume and longer survival duration produced far more labeled cells in the FEF, as well as labeling in adjacent cortical areas (Table 1, Case 6; Figs. 5A, 6A, and 7G). However, inspection of the deep cerebellar nuclei revealed a surprising lack of cerebellotectal neurons expressing fluorescent proteins in the rAAV2-Retro-CAG cases (Fig. 5C, F and Fig.7C, F). In contrast, the deep cerebellar nuclei of the animal injected with rAAV2-Retro-hSyn-hChR2(H134R)-GFP were heavily labeled (Fig. 6C and Fig. 7I). The labeled cerebellotectal neurons were found in all the deep cerebellar nuclei contralateral to the injection site. These results are summarized in Table 3, and again suggest that the AAV capsid, while permissive for broad cell-type infectivity demonstrates cell type-specific transduction solely based on the capsid/promoter combination.

DISCUSSION

This study expands upon our recently published novel observation that AAV capsid-promoter interactions can directly influence AAV cell-specific gene expression within the rat CNS.[11] In addition to CBA and Cbh promoters, these findings extend this observation by establishing an AAV9 capsid-promoter interaction with the clinically utilized JetI, a ubiquitous minimal synthetic promoter. In the rat striatum, AAV9-JetI-GFP vectors exhibited predominantly oligodendrocyte gene expression over neuronal gene expression. However, insertion of 6 alanines into VP1/VP2 of the AAV9 (AAV9AU) capsid as previously described[11] significantly shifted the gene expression from oligodendrocytes to neurons. This AAV9AU capsid-induced shift in cellular gene expression recapitulates a similar AAV9AU capsid influence on cellular gene expression previously found for the Cbh promoter.[11] Critical to these experiments

Figure 2. Chartings from a case illustrating neuronal labeling following injections of rAAV2-Retro-CAG-GFP injected into the FEF of a rhesus macaque monkey. *Red dots* indicate the approximate location and density of neurons within example sections. Scale bar in **B** is true for all presented sections. III, oculomotor nucleus; IV, trochlear nucleus; *ac*, anterior commissure; AM, anteromedial thalamic nucleus; Amy, amygdala; asp, arcuate spur; BIC, brachium of the inferior colliculus; C, caudate; CA, cerebral aqueduct; *cc*, corpus callosum; Cd, caudate nucleus; CG, cingulate gyrus; Cl, claustrum; cs, central sulcus; D, dentate nucleus; DR, dorsal raphe; F, fastigial nucleus; FEF, frontal eye field (Area 8); GPe, external segment of the globus pallidus; GPi, internal segment of the globus pallidus; Hc, hippocampus; I, interposed nuclei; ia, inferior arcuate sulcus; *ic*, internal capsule; IC, inferior colliculus; its, inferior temporal sulcus; ll, lateral lemniscus; LGN, lateral geniculate nucleus; ls, lateral sulcus; LV, lateral ventricle; mcp, middle cerebellar peduncle; MD, mediodorsal thalamic nucleus; ml, medial lemniscus; mlf, medial longitudinal fasciculus; MR, median raphe nucleus; ot, optic tract; *ox*, optic chiasm; P, putamen; PAG, periaqueductal gray; PGr, pontine gray; *py*, pyramids; RN, red nucleus; RTP, reticulotegmental pontine nucleus; sa, superior arcuate sulcus; SC, superior colliculus; scp, superior cerebellar peduncle; SEF, supplementary eye field; SN, substantia nigra; ST, subthalamic nucleus; sts, superior temporal sulcus; VPL, ventroposterolateral thalamic nuclei; VPM, ventroposteromedial thalamic nuclei; ZI, zona incerta.

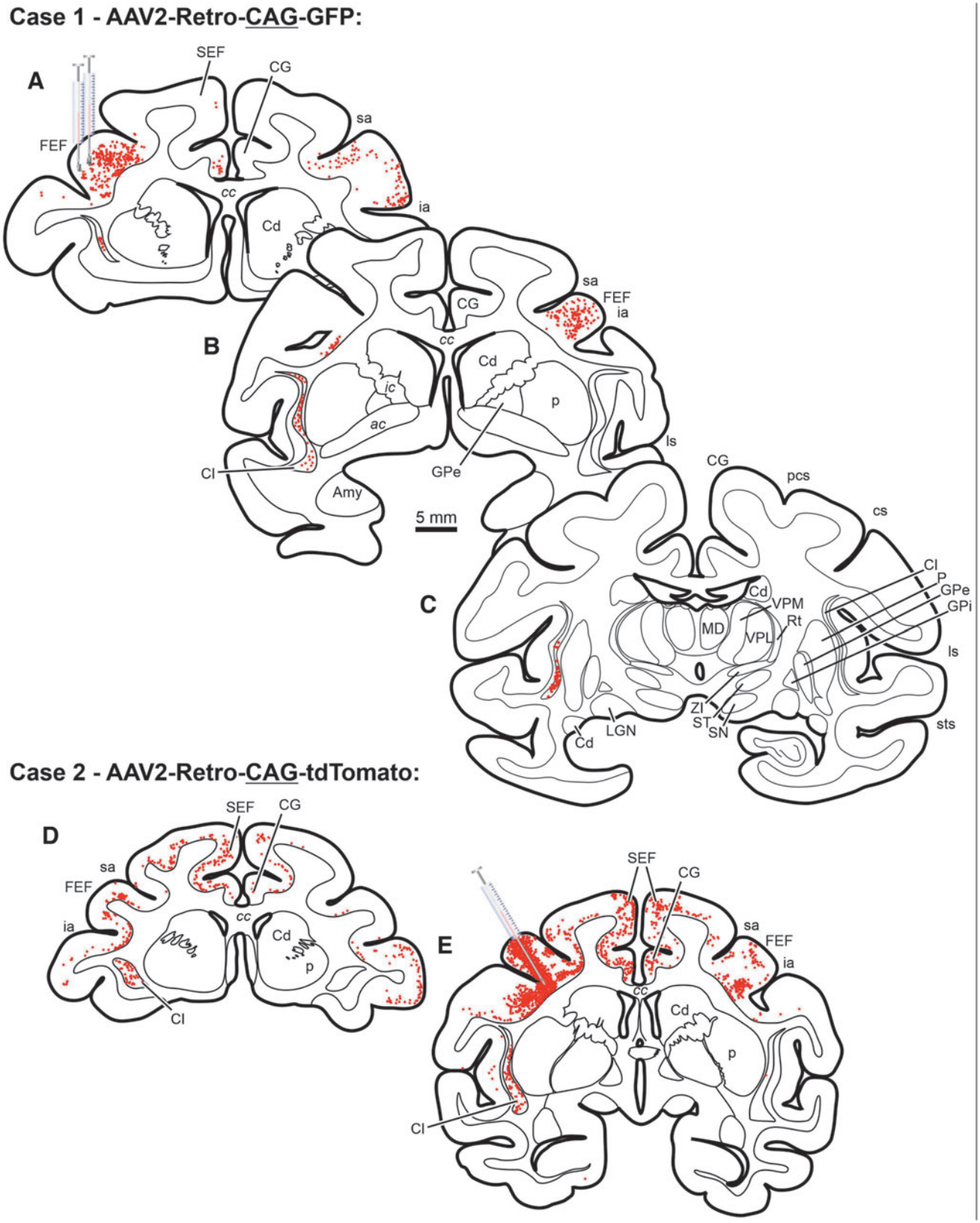
Case 1 - AAV2-Retro-CAG-GFP:
A
SEF
CG
FEF
sa
cc
ia
Cd
B
sa
FEF
ia
CG
cc
Cd
ic
p
ac
ls
Cl
GPe
Amy
5 mm
C
CG
pcs
cs
Cl
P
GPe
GPi
Cd
VPM
Rt
MD
VPL
ls
ZI
ST
SN
sts
Cd
LGN
Case 2 - AAV2-Retro-CAG-tdTomato:
D
SEF
CG
sa
FEF
ia
cc
Cd
p
Cl
E
SEF
CG
sa
FEF
ia
cc
Cd
p
Cl

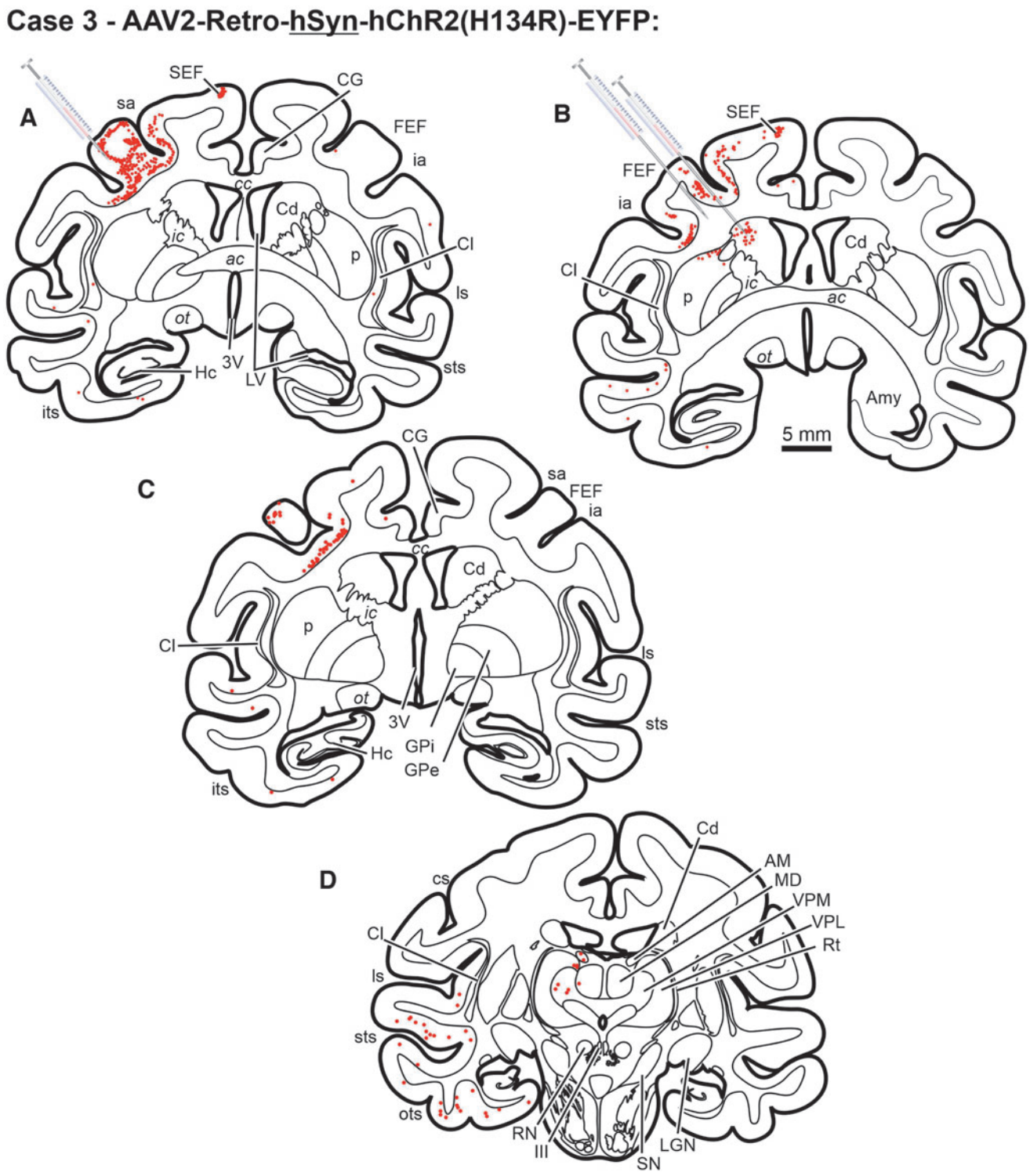

Figure 3. Chartings from a case illustrating neuronal labeling following injections of rAAV2-Retro-hSyn-hChR2(H134R)-EYFP injected into the FEF of a rhesus macaque monkey **(A–D)**. *Red dots* indicate the approximate location and density of neurons within example sections. Scale bar in B is true for all presented sections.

is the fact that Powell *et al.*[11] also established that the alanine insertion did not alter the ability of AAV9 to gain access to oligodendrocytes. As a result of these previously published data combined with the above JetI combination, it is clear that this *in vivo* AAV9 capsid-promoter interaction translates yet to another promoter (*i.e.*, synthetic) and may be a widespread phenomena subject to various AAV capsid/promoter combinations.

Previous efforts looking at AAV capsid library have demonstrated novel new reagents, but in some cases,

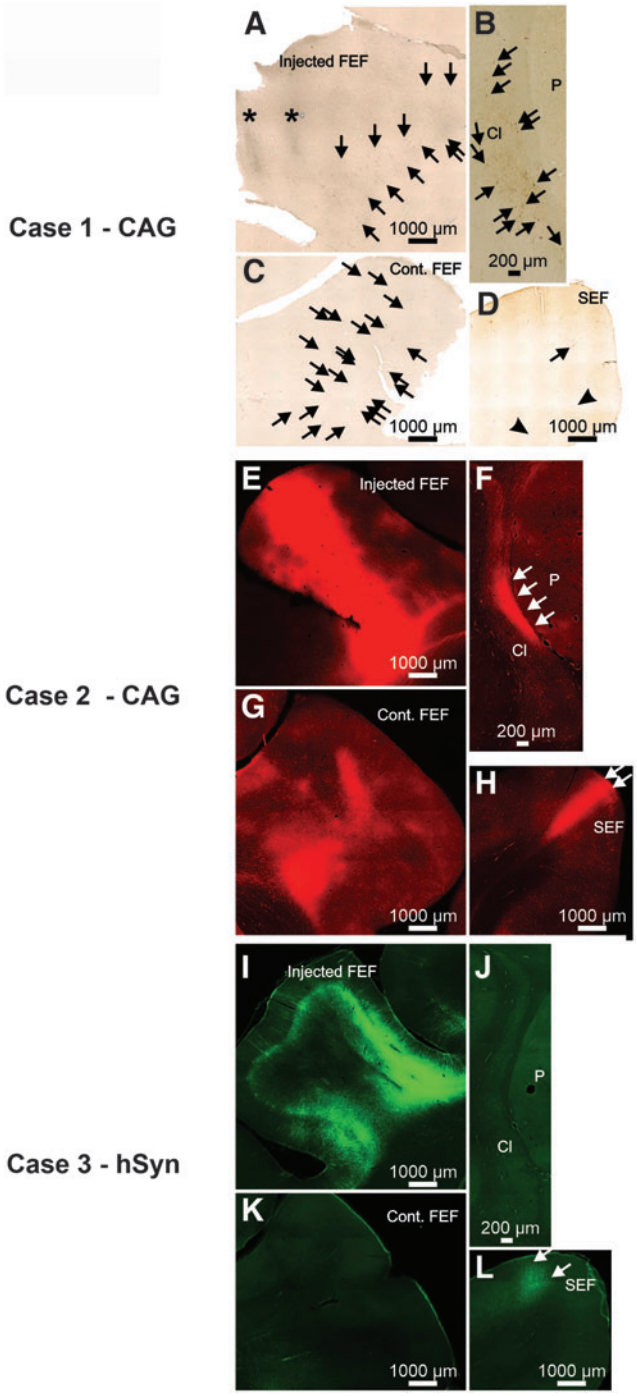

Figure 4. Photomicrographs from Case 1 **(A–D)**, 2 **(E–H)**, and 3 **(I–L)** illustrating neuronal labeling provided by AAV2-retro-CAG (primate Cases 1 and 2) or AAV2-retrohSyn following injections into the FEF. *Asterisk* indicates the location of needle tracts. *Arrows* indicate locations of individual neurons in photomicrographs where it may not be obvious to the observer.

species-specific isolation of AAV vectors that do not translate to larger animal models.[36] These nonhuman primate findings further suggest that this CNS capsid-promoter interaction not only occurs in another species but also with a different AAV capsid. All vector constructs were packaged with the rAAV2-Retro capsid, so the efficiency of *in vivo* retrograde transport would be expected to be the same across the two different promoter constructs. For the FEF injections, the CAG expression vectors supported robust retrograde expression in the contralateral FEF and ipsilateral claustrum, while the hSyn expression vectors did not exhibit retrograde gene expression in these structures. One possible explanation for these results could involve different virus titers and survival times (Table 1). However, for the FEF injections, the CAG vector injections were lower in titer and shorter in survival time compared to the hSyn vector injections. Given these injection differences, and the similar capsid uptake at the site of injection, one would expect more retrograde labeling from the hSyn vector compared to the CAG vector. Clearly, the fact that substantially more retrograde labeling was produced by the CAG vector suggests that parameter differences did not contribute to the observed differences in gene expression levels. Also, given that the hSyn is an endogenous promoter and exhibited substantial gene expression at the site of injection, it appears that promoter silencing likely was not a factor. Therefore, these data support our conclusion that the rAAV2-Retro capsid interacted with the hSyn promoter to suppress gene expression in the contralateral FEF and ipsilateral claustrum.

Prior experience suggests that one needs to invoke caution when working in large animal models where experimental conditions are not totally identical. However, even in light of differences in injection parameters, the SC data also suggest capsid-promoter interactions. For example, similar to the FEF study, both vectors supported gene expression at the injection site and in the retrogradely labeled corticotectal neurons within the FEF. Although the level of FEF expression was markedly different between the two vectors, this difference could be attributed to the larger injection volume and the longer survival duration for the hSyn vector (Table 1). Importantly, however, the pattern of labeling for both the injection site and the retrograde labeling within the FEF was present for all three cases. In contrast, the hSyn vector also supported robust expression in the retrogradely labeled cerebellotectal neurons, while two independent cases where the CAG vector was injected into the SC failed to show retrograde labeling in the deep cerebellar nuclei, even though CAG driven expression in Case 5 was similar to hSyn-driven expression in Case 6 (Fig. 7). These observations provide further evidence supporting the idea that capsid-promoter interactions are taking place across species and capsids, and along the neuroaxis.

Generally, studies of intraparenchymal AAV injections in the primate CNS have suggested that gene expression in specific neuronal populations depends upon the promoter and, in many instances, promoters only determine the degree of transgene expression. For example, Watakabe *et al.*[37] compared local transduction using AAV1-CaMKII

Table 2. *Summary of frontal eye field data*

Construct	*Injection Site Labeling*	*SEF*	*Claustrum*	*Contralateral FEF*	*MD Thal.*	*Fig. Ref.*
rAAV2-Retro-CAG-GFP	Yes	Yes	Yes	Yes	No	Figure 2A–C
rAAV2-Retro-hSyn-hChR2(H134R)-EYFP	Yes	Yes	No	No	No	Figure 3A–D

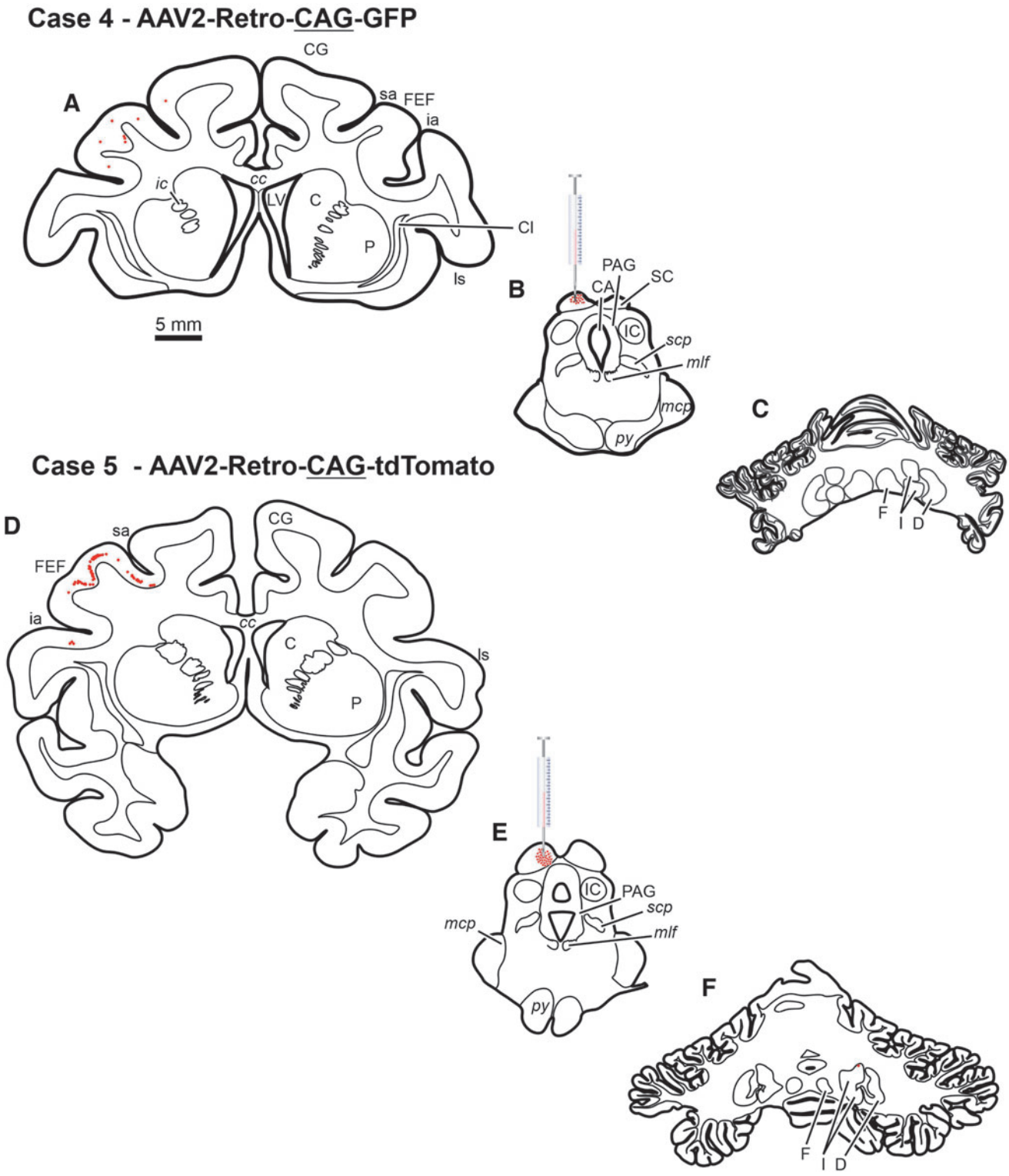

Figure 5. Chartings from two cases illustrating neuronal labeling following injections of rAAV2-Retro-CAG-GFP (Case 1, **A–C**) (Case 2, **D–F**) that were placed into the SC of two rhesus macaque monkeys. *Red dots* indicate the approximate location and density of neurons within example sections. Scale bar in A is true for all presented sections.

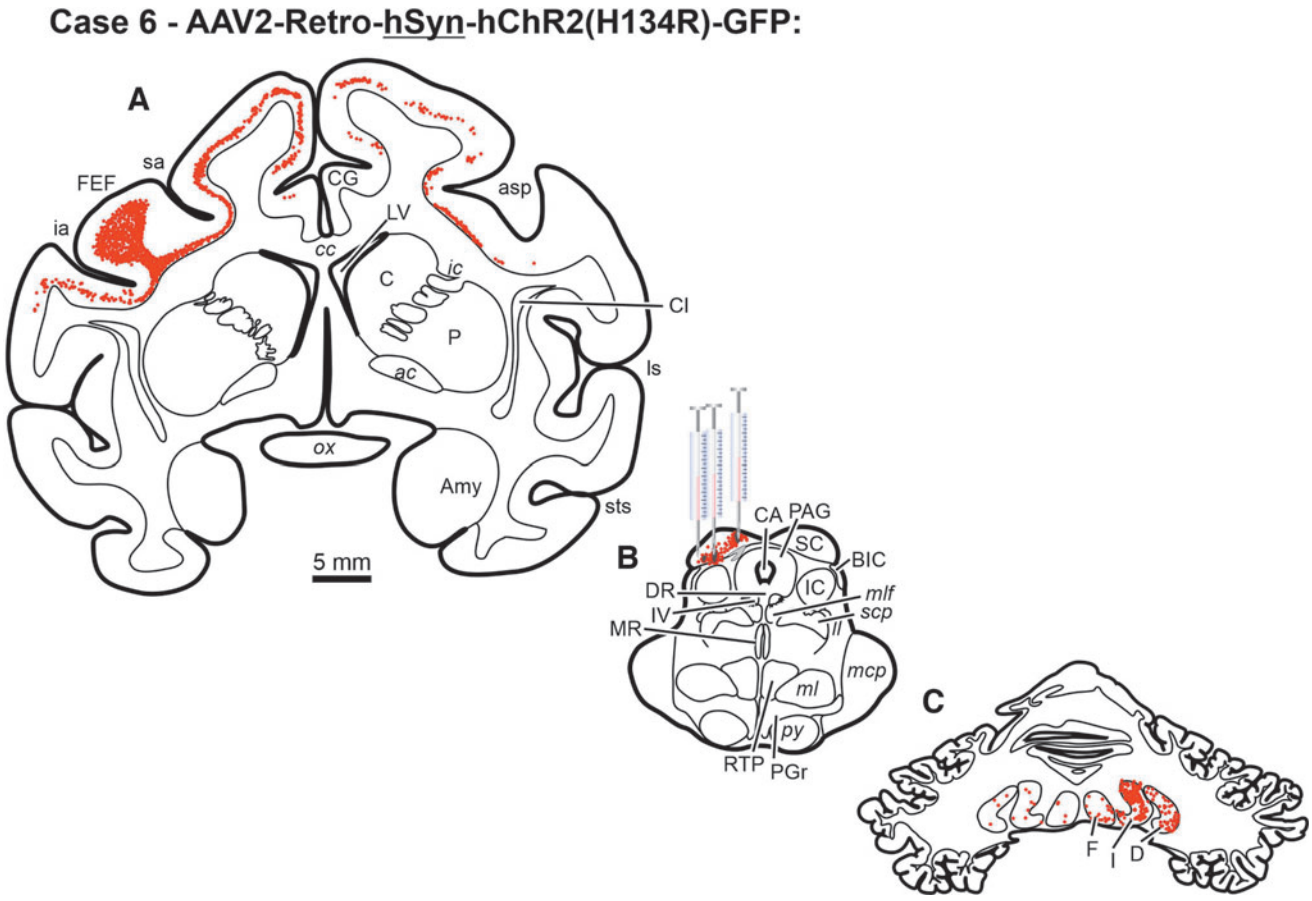

Figure 6. Chartings from a case illustrating neuronal labeling following injections of rAAV2-Retro-hSyn-hChR2(H134R)-GFP **(A–C)** placed into the SC of a rhesus macaque monkey. *Red dots* indicate the approximate location and density of neurons within example sections. Scale bar in A is true for all presented sections.

and AAV1-Syn1 to AAV9-CaMKII and AAV9-Syn1 in marmosets. They concluded that the only difference between the two promoters was the degree of transgene expression. In contrast, this study suggests that capsid-promoter interactions can also affect the pattern of transgene expression, not just the amount of labeling. With the current focus upon generating novel AAV capsids in nonhuman primates and rodents, the possibility exists that novel transduction properties arise not only from unique capsid binding properties but also from unknown novel capsid-promoter interactions. It is tempting to suggest that this unique observation that we have documented may not be restricted to AAV capsid/promoter interactions in the brain, but in peripheral tissue also.

Additional analytical experiments are required where vector DNA *in situ* analysis, genome copy number, mRNA levels, and persistent expression are scrutinized beyond the level carried out in these initial studies. More importantly, recent data using cell base assays and siRNA library approach have resulted in identification of cellular factors that are linked with AAV vector transcription and in one case bound to AAV capsid.[38] While these efforts apparently identify cellular protein candidates that impact all AAV serotypes for gene expression after vector infection and uncoating in the nucleus, the observations we have documented appear to be cell type specific (*e.g.*, neurons vs. oligos), promoter specific (CBA vs. CAG), and strongly influenced by subtle amino acid changes in the unique region of minor AAV structural proteins Vp1 and 2 (*e.g.*, AAV9 AU). Therefore unlike cell-based ''knockdown'' assays, future mechanistic studies to unravel these current observations will require *in vivo* analysis. In an effort to establish the overall contribution of this novel interaction between the AAV capsid and its genomic cargo, certain attributes of the AAV lifecycle may shed light on these phenomena: namely viral latency. AAV is known to have a biphasic lifecycle consisting of lytic when Ad helper is present and latent when absent. Under certain conditions, AAV would be permissive for all steps involved in lytic infection, including receptor binding, trafficking, and nuclear entry with viral genomes finally being retained in a conformation not suited for transgene expression. The data derived in both our rodent and primate studies suggest that various AAV capsid/promoter combinations may result in latent genomes, where all steps of virus permissivity take place, except the last step of gene expression. Noteworthy,

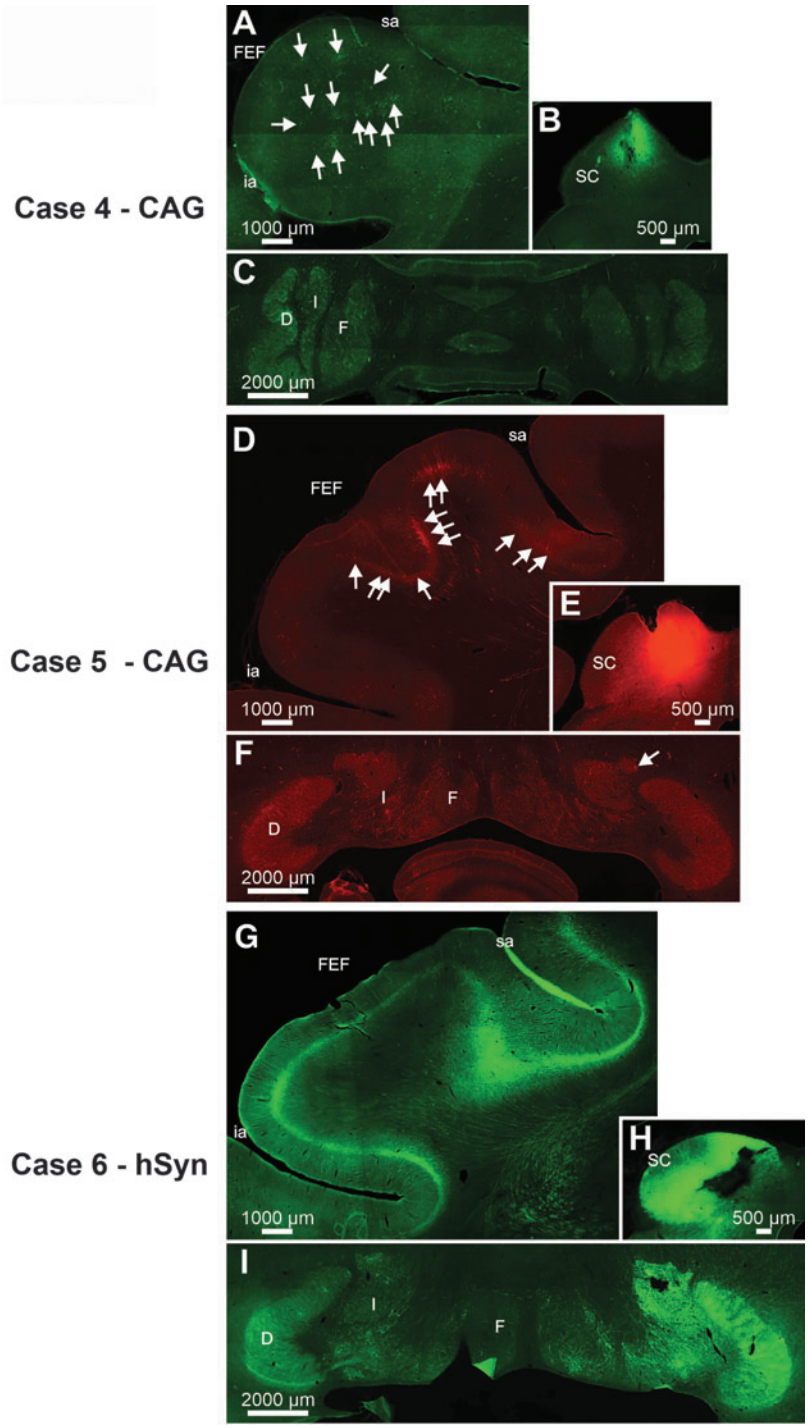

Figure 7. Photomicrographs from Cases 4 **(A–C)**, 5 **(D–F)**, and 6 **(G–I)** illustrating neuronal labeling provided by AAV2-retro-CAG (Cases 4 and 5) or AAV2-retro-hSyn (Case 6) following injections into the SC. *Arrows* indicate locations of individual neurons in photomicrographs where it may not be obvious to the observer.

Table 3. *Summary of superior colliculus data*

Construct	*Injection Site Labeling*	*FEF*	*Deep Cerebellar Nuclei*	*Fig. Ref.*
rAAV2-Retro-CAG-GFP	Yes	Yes	No	Figure 4A–C
rAAV2-Retro-CAG-GFP	Yes	Yes	No	Figure 4D–F
rAAV2-Retro-hSyn-hChR2(H134R)-GFP	Yes	Yes	Yes	Figure 5A–C

studies by Muzyczka et al.[39] have identified a region on the AAV capsid that when mutated carry out all steps of infection, including uncoating, but remain negative for gene expression illustrating precedence for such a phenomena. Irrespective of mechanism, we document a unique attribute of AAV vectors in both rodent and primate models that until recently remained undescribed: namely capsid/promoter interactions, which dictated cell type transduction profiles regardless of virus permissivity. While these observations may be aligned with aspects of AAV latency, they create potential consternation with respect to influence on AAV viral vectors for human gene therapy and may pose a health risk when transitioning from animal model to human clinical studies.

ACKNOWLEDGMENTS

We are grateful to Dr. Paul J. May for his technical expertise in processing some of the tissues included in this study and for his critical commentary on the article. We also thank Dr. Steven Gray for providing the JetI promoter plasmid.

AUTHORS' CONTRIBUTIONS

S.K.P. created and produced the AAV vectors for the rat study, T.J.M. conducted the rat study, M.O.B., H.G.E., T.D., M.A.B., and M.A.B. conducted the NHP studies, and M.O.B., T.J.M., M.A.S., and R.J.S. wrote and or edited the article.

AUTHOR DISCLOSURE

R.J.S. is a founder and a shareholder at Asklepios Biopharmaceutical. He holds patents that have been licensed by UNC to Asklepios Biopharmaceutical, for which he receives royalties. The other authors report no conflicts of interest.

FUNDING INFORMATION

This work was supported by The Hartwell Biomedical Research Fellowship (M.O.B.), the Duke Institute for Brain Sciences Germinator Award (M.O.B. and M.A.S.), NIH grant NEI R21 EY030278 (M.A.S.), NIH grant EY013692 (M.A.B.), and NIH grant NINDS NS082289 (T.J.M.). NINDS grant NS082289 (T.J.M.). Rat confocal microscopy was conducted in the UNC Neuroscience Center Confocal and Multiphoton Imaging Core (NINDS center grant P30 NS045892).

SUPPLEMENTARY MATERIAL

Supplementary Figure S1
Supplementary Figure S2

REFERENCES

1. Mendell JR, Al-Zaidy S, Shell R, et al. Single-dose gene-replacement therapy for spinal muscular atrophy. N Engl J Med 2017;377:1713–1722.
2. Bailey RM, Armao D, Nagabhushan Kalburgi S, et al. Development of intrathecal AAV9 gene therapy for giant axonal neuropathy. Mol Ther Methods Clin Dev 2018;9:160–171.
3. El-Shamayleh Y, Horwitz GD. Primate optogenetics: progress and prognosis. Proc Natl Acad Sci U S A 2019;116:26195–26203.
4. Galvan A, Caiola MJ, Albaugh DL. Advances in optogenetic and chemogenetic methods to study brain circuits in non-human primates. J Neural Transm (Vienna) 2018;125:547–563.
5. Galvan A, Stauffer WR, Acker L, et al. Nonhuman primate optogenetics: recent advances and future directions. J Neurosci 2017;37:10894–10903.
6. Haggerty DL, Grecco GG, Reeves KC, et al. Adeno-associated viral vectors in neuroscience research. Mol Ther Methods Clin Dev 2020;17:69–82.
7. Asokan A, Schaffer DV, Samulski RJ. The AAV vector toolkit: poised at the clinical crossroads. Mol Ther 2012;20:699–708.
8. Dimidschstein J, Chen Q, Tremblay R, et al. A viral strategy for targeting and manipulating interneurons across vertebrate species. Nat Neurosci 2016;19:1743–1749.
9. Grimm D, Buning H. Small but increasingly mighty: latest advances in AAV vector research, design, and evolution. Hum Gene Ther 2017;28:1075–1086.
10. Tervo DG, Hwang BY, Viswanathan S, et al. A designer AAV variant permits efficient retrograde access to projection neurons. Neuron 2016;92:372–382.
11. Powell SK, Samulski RJ, McCown TJ. AAV capsid-promoter interactions determine CNS cellselective gene expression in vivo. Mol Ther 2020;28:1373–1380.
12. Haberman R, Criswell H, Snowdy S, et al. Therapeutic liabilities of in vivo viral vector tropism: adeno-associated virus vectors, NMDAR1 antisense, and focal seizure sensitivity. Mol Ther 2002;6:495–500.
13. Karumuthil-Melethil S, Nagabhushan Kalburgi S, Thompson P, et al. Novel vector design and hexosaminidase variant enabling self-complementary adeno-associated virus for the treatment of Tay-Sachs Disease. Hum Gene Ther 2016;27:509–521.
14. Huerta MF, Kaas JH. Supplementary eye field as defined by intracortical microstimulation: connections in macaques. J Comp Neurol 1990;293:299–330.
15. Huerta MF, Krubitzer LA, Kaas JH. Frontal eye field as defined by intracortical microstimulation in squirrel monkeys, owl monkeys, and macaque monkeys. II. Cortical connections. J Comp Neurol 1987;265:332–361.
16. Leichnetz GR, Goldberg ME. Higher centers concerned with eye movement and visual attention: cerebral cortex and thalamus. Rev Oculomot Res 1988;2:365–429.
17. Kurimoto Y, Kawaguchi S, Murata M. Cerebellotectal projection in the rat: anterograde and retrograde WGA-HRP study of individual cerebellar nuclei. Neurosci Res 1995;22:57–71.
18. May PJ, Hartwich-Young R, Nelson J, et al. Cerebellotectal pathways in the macaque: implications for collicular generation of saccades. Neuroscience 1990;36:305–324.

19. May PJ, Hall WC. The cerebellotectal pathway in the grey squirrel. Exp Brain Res 1986;65:200–212.

20. Kawamura S, Hattori S, Higo S, et al. The cerebellar projections to the superior colliculus and pretectum in the cat: an autoradiographic and horseradish peroxidase study. Neuroscience 1982; 7:1673–1689.

21. Hirai T, Onodera S, Kawamura K. Cerebellotectal projections studied in cats with horseradish peroxidase or tritiated amino acids axonal transport. Exp Brain Res 1982;48:1–12.

22. Cushnie AK, El-Nahal HG, Bohlen MO, et al. Using rAAV2-retro in rhesus macaques: promise and caveats for circuit manipulation. J Neurosci Methods 2020;345:108859.

23. Weinberg MS, Criswell HE, Powell SK, et al. Viral vector reprogramming of adult resident striatal oligodendrocytes into functional neurons. Mol Ther 2017;25:928–934.

24. Paxinos G, Watson C. The Rat Brain in Stereotaxic Coordinates. San Diego: Academic Press, 1998.

25. Lee WH, Lisanby SH, Laine AF, et al. Minimum electric field exposure for seizure induction with electroconvulsive therapy and magnetic seizure therapy. Neuropsychopharmacology 2017;42: 1192–1200.

26. Lee WH, Lisanby SH, Laine AF, et al. Electric field model of transcranial electric stimulation in nonhuman primates: correspondence to individual motor threshold. IEEE Trans Biomed Eng 2015;62: 2095–2105.

27. Peterchev AV, Jalinous R, Lisanby SH. A transcranial magnetic stimulator inducing near-rectangular pulses with controllable pulse width (cTMS). IEEE Trans Biomed Eng 2008;55:257–266.

28. Peterchev AV, Krystal AD, Rosa MA, et al. Individualized low-amplitude seizure therapy: minimizing current for electroconvulsive therapy and magnetic seizure therapy. Neuropsychopharmacology 2015;40:2076–2084.

29. Grimaldi P, Cho SH, Lau H, et al. Superior colliculus signals decisions rather than confidence: analysis of single neurons. J Neurophysiol 2018; 120:2614–2629.

30. Odegaard B, Grimaldi P, Cho SH, et al. Superior colliculus neuronal ensemble activity signals optimal rather than subjective confidence. Proc Natl Acad Sci U S A 2018;115:E1588–E1597.

31. Crapse TB, Lau H, Basso MA. A role for the superior colliculus in decision criteria. Neuron 2018; 97:181–194 e186.

32. Bohlen MO, El-Nahal HG, Sommer MA. Transduction of craniofacial motoneurons following intramuscular injections of canine adenovirus type-2 (CAV-2) in rhesus macaques. Front Neuroanat 2019;13.

33. Weiss AR, Liguore WA, Domire JS, et al. Intrastriatal AAV2.retro administration leads to extensive retrograde transport in the rhesus macaque brain: implications for disease modeling and therapeutic development. Sci Rep 2020;10: 6970. DOI: 10.1038/s41598-020-63559-7.

34. Huerta MF, Krubitzer LA, Kaas JH. Frontal eye field as defined by intracortical microstimulation in squirrel monkeys, owl monkeys, and macaque monkeys: I. Subcortical connections. J Comp Neurol 1986;253:415–439.

35. Tian JR, Lynch JC. Subcortical input to the smooth and saccadic eye movement subregions of the frontal eye field in Cebus monkey. J Neurosci 1997;17:9233–9247.

36. Matsuzaki Y, Konno A, Mochizaki R, et al. Intravenous administration of the adeno-associated virus-PHP.B capsid fails to upregulate transduction efficiency in the marmoset brain. Neurosci Lett 2018;665:182–188.

37. Watakabe A, Ohtsuka M, Kinoshita M, et al. Comparative analyses of adeno-associated viral vector serotypes 1, 2, 5, 8 and 9 in marmoset, mouse and macaque cerebral cortex. Neurosci Res 2015;93:144–157.

38. Schreiber CA, Sakuma T, Izauiya Y, et al. An siRNA screen identifies the U2 snRNP spliceosome as a host restriction factor for recombinant adeno-associated viruses. PLoS Pathogens 2015;11:e1005082.

39. Aydemir F, Salganik M, Resztak J, et al. Mutants at the 2-fold interface of adeno-associated virus type 2 (AAV2) structural proteins suggest a role in viral transcription for AAV capsids. J Virol 2016;90:7196–7204.

Received for publication July 7, 2020;
accepted after revision September 3, 2020.

Published online: September 16, 2020.